Singh, J Material Sci Eng 2019, 8:1
DOI: 10.4172/2169-0022.1000507

Journal of Material Sciences & Engineering

Research Article Open Access

Finite Element Analysis of Chemical Assisted Ultrasonic Machining Process to Investigate the Effect of Abrasive on Polycarbonate (UL-752) Glass and USM Tool

Kanwal Jit Singh*

Department of Mechanical Engineering, Giani Zail Singh Campus College of Engineering and Technology, Punjab India

Abstract

In this research paper, the Finite Element Analysis is used for the investigation. The modal of polycarbonate bullet proof glass and the abrasive particle is prepared to study the effect of machining mechanism. Through analysis, it concludes that hard abrasive gives the large stressed zone, which increases the material removal rate. In this experimental study, Boron carbide abrasive gives better material removal rate as compared to Silicon carbide and Alumina Abrasive. It also observed from the analysis, higher material removal rate also encourage the tool wear rate. Boron carbide gives higher tool wear rate as compare to other abrasive. The results are verified with the experimentation, it gives the approximately same results of Finite Element Analysis.

Keywords: Finite element analysis; Ultrasonic; Polycarbonate; Glass; Chemical-assisted Ultrasonic Machining; Finite Element Method (FEM)

Introduction

Ultrasonic components can be turned using equation based on theory derived from the longitudinal vibration of rod. Simple geometric shapes can be turned accurately using this method, but as the geometry of the blade increases, complexity analytical solutions are ineffective. Very complex component geometries can be turned accurately using the computational FE method.

The creation of the finite element method was invented in 1943 by Courant, who obtained approximate solution to vibration system by utilizing the Ritz method of numerical analysis and minimization of variational calculus. Further work followed this pioneering work by Courant to establish the FE method for practical use. In 1970s it was being used by large industries such as aerospace, automotive, defense and nuclear industries at large, mainframe computers. However, with rapid advancements in computational power and the reduced cost of FE software, FEA is now widely used by many industries. [1,2]. The FE method works by modelling a structure using a mesh of elements connected together using nodes [3]. These elements can have simple as well as complex material properties applied to characterize the behaviour of the structure under analysis [2]. Boundary and load conditions can be simulated on the nodes or elements of the mesh and a variety of analytical results can be calculated depending on the type of analysis required by the researcher and the parameters the researcher is interested in. Several modelling techniques can be used to analyze a structure in using a 2D or 3D modelling domain, the choice of which depends on deployment the FE methods. FEA is now considered to be an essential tool in the arsenal of an engineer's especially for design or troubleshooting [1].

The history of the ultrasonic machining began by Mr. RW Wool and Mr. AL Loomis in 1927 with publishing a paper on USM. In 1954, first time USM come into the existence, when Mr. L Balamuth was approved first patent for USM. According to British patent number 602801 (1945) which was issued to an American engineer Mr. L Balamuth, who discovered USM in 1942, while he was investigating the dispersion of solid in liquid by mean of a magnetostrictively vibration nickel tube. In 1945, first time Mr. JO Farrer proposed the utilization of USM. In 1962, the USA was issued USM process patent under number 2560716.

In USM, low frequency 50 Hz (c/s) input signal is converted into high frequency (15 kHz to 30 kHz) output electric signal. Then, these electrical signals are transferred in the liner mechanical vibrations through magnetostrictive or piezoelectric transducer or booster combination. Magnetostrictive transducers are found in old USM, and these are less effective due to high eddy current losses and high heat generation. They require additional cooling resources to reduce the heating effects. Piezoelectric transducers are more effective and efficient, as these tarnsducesr have less energy losses and do not require additional cooling sources. Liner mechanical energy is then transmitted on to energy focusing as well as amplifying device known as horn or sonotrode. USM horn causes the USM tool to vibrate along its longitudinal axis at sonic frequency, usually greater than 20,000 Hz, with an amplitude of 12-50 μm [4,5]. It has 50 to 3000 W power rating for feeding in longitudinal direction, with controlled static load applied on the tool. The power supply rating for USM is usually: potential=220 volts and current=12A.

The mixture of abrasive particles and carrying medium known as abrasive slurry is supplied in between the tool and work-piece at the rate of 30-35 litre/min. Various types of abrasives used in USM are silicon carbide (SiC), boron carbide (B_4C), alumina (Al_2O_3) and diamond dust. Water and some other suitable carrying mediums are utilized in abrasive slurry preparation. The sonic frequency vibrations of USM tool are transmitted on to the abrasive particles held in the slurry and slurry particles impact over the work surface. The bombardment of the abrasive slurry starts eroding the material in that particular area through micro-chipping. These microchips are flushed with the carrying medium. USM process is a non-heat effected

***Corresponding author:** Kanwal Jit Singh, Department of Mechanical Engineering, Giani Zail Singh Campus College of Engineering and Technology, Punjab India, Tel: +918054666123; E-mail: Khalsa.kanwal@yahoo.com

Received January 08, 2019; **Accepted** January 17, 2019; **Published** January 27, 2019

Citation: Singh KJ (2019) Finite Element Analysis of Chemical Assisted Ultrasonic Machining Process to Investigate the Effect of Abrasive on Polycarbonate (UL-752) Glass and USM Tool. J Material Sci Eng 8: 507. doi: 10.4172/2169-0022.1000507

Citation: Singh KJ (2019) Finite Element Analysis of Chemical Assisted Ultrasonic Machining Process to Investigate the Effect of Abrasive on Polycarbonate (UL-752) Glass and USM Tool. J Material Sci Eng 8: 507. doi: 10.4172/2169-0022.1000507

zone, non-residual stress and non-thermal stress produced machining process [6-9].

USM process has generally involves low material removal rate; however the applications of USM process are not limited. USM process is applicable for metal, non-metal, ceramics and composite materials. USM process is non-thermal and non-chemical affected machining process, so that the processed materials are not effected either metallurgically or chemically. USM process is also preferable for producing micro holes as small as 50 µm in diameter, can be easily drilled. The depth to diameter ratio is limited to 3:1 [10,11]. For effective ultrasonic machining, tool and horn must be designed with given mass and shape consideration so that resonance can be achieved with in frequency range capability of the USM [12-14].

Design Process for Ultrasonic Modelling

The literature on ultrasonic component design indicates that, for uniform cylinder, the gain of the turned component is 1, that is, theoretically, if 1 micron amplitude is supplied by the transducer at one end of the rod, then the displacement at the other end is 1 micron. This however never occurs in reality due to some internal losses. Also, gain is dependent on the rate of change in cross-sectional area from the base of the component, when the input is supplied to the tip. A reduction in cross-sectional area from the base to the tip increases the gain and an increase in cross-sectional area reduces the gain. Many components profiles exist such as conical, exponential, stepped or combination of these, to magnify or reduce amplitude at the tip of the component [15-17].

During the experiment, the cutting tool is turned to the longitudinal mode of vibration at 30 kHz frequency, material alloy steel (High Speed Steel) and work-piece (Polycarbonate bullet proof glass). An increase in gain allows a large range of amplitude to be investigated. To increase the vibration amplitude of the tool, two symmetric circular cuts were taken along the longitudinal axis to reduce the cross sectional area from the base to the tip of the tool as shown in Figure 1.

Stress Analysis using FEA

After the tool has been turned, a vibrating force was applied on it as indicated in Equation 1

$$F=A \sin \omega t \qquad (1)$$

Where; F=Force; A=Amplitude (8 microns); ω=Natural Frequecny; t=Time.

A steady-state dynamic analysis provides the steady-state amplitude and phase of the response of a system due to harmonic excitation at a given frequency. This analysis has been carried out using ABAQUS software that allows direct-solution steady-state dynamic procedure to conduct the frequency sweep. The frequency sweep was applied by loading at a series of different frequencies and recording the resulting responses (stresses produced) appropriately.

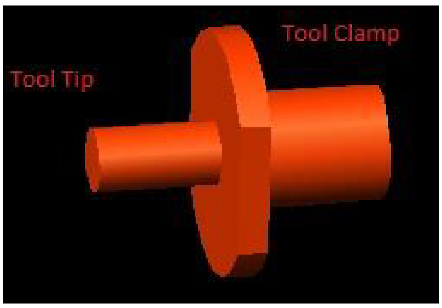

Figure 1: Symmetric circular cuts through a uniform rod.

The stress distribution in the tool can be plotted using the Von-mises and Hencky criteria as shown in Equation 2 given below, where σ_1, σ_2, σ_3 are the principle stresses and σ_o is the yield stress [18-21].

$$(\sigma_1-\sigma_2)^2+ (\sigma 2- \sigma_3)^2+(\sigma 3-\sigma_1)^2=2\,\sigma_o^2 \qquad (2)$$

Assuming that the stress distribution lies in-plane along the cross-section of the tool, where no traverse movement exists. This implies that there is only one principle stress (σ_2) that always acts in one direction, with no shear stress, as shown in eqn (3). [18,19,22-24].

$$\sigma_1,\ \sigma_3=0$$

$$(0-\sigma_2)^2+(\sigma_2-0)^2+0=2\,\sigma_o^2$$

$$\sigma_2^2=2\,\sigma_0^2$$

$$\sigma_2=\sigma_0 \qquad (3)$$

Thus, the Von Mises stress will be the same as the maximum principle stress in the longitudinal direction of wave guides. The maximum stress limits of components must always be considered in any design, and for ultrasonic tool ideally the maximum stress must lie in the elastic region of the material. The maximum allowable stress in an ultrasonic component can be considered as the yield stress.

s of the material divided by the safety factor as denoted in eqn. (4) [18,19].

$$\sigma_{max}=\frac{\sigma_{yield}}{Safety\ Factor} \qquad (4)$$

Selection for the Workpiece and USM Tool

Material selection for ultrasonic components has been critical to ensure that tool operates correctly. Various material characteristics such as high strength and high toughness are generally required for the design of ultrasonic components especially for the ultrasonic tool. Minimizing heat generation during operation is often a design specification for ultrasonic tool to restrict burning at the cut interface that can ruin the substrate material. Further, the materials with low internal friction co-efficient are required to minimize temperature rise during operation. However, in some processes, such as ultrasonic machining of glass, a slight increase in temperature is sometimes an advantage. Whereas for softer materials marginal increase in temperature can locally melt the material at the interface, which can often produce a cut surface, which can be sean in the form of a bead (ultrasonic welding defect) to naked eye. This can be avoided by adding a washer in between the metal to metal interfaces.

Ideally during USM operation, zero acoustic loss factor is highly desirable, as there should not be any energy losses due to heat or noise, and all the energy supplied will be transformed into mechanical vibrations. But in reality every ultrasonic component will experience acoustic losses and energy is lost in the system. Often the quality factor is used to characterize the effectiveness of the ultrasonic components and a high mechanical Q is often advantageous for ultrasonic components design. The mechanical Q or quality factor can be calculated using eqn. (5), where Q is the quality factor and Φ is the acoustic loss available from material table [22].

$$Q=1/\Phi \qquad (5)$$

Many materials have high quality factor, but it is also critical when selecting a material for component design to consider the acoustic impedance (Z) of the material, which can be determined from Equation 6, where c is the speed of sound in the material and ρ is the density of the material [22,25].

$$Z=c\,\rho \tag{6}$$

When several ultrasonic components are connected, usually by using threaded studs where one component is tightened against another, the acoustic impedance should be matched as closely as possible to ensure transfer is maximized between joining components and to ensure the vibrations are transferred effectively from one component to the next [26].

Boundary Condition and Loads

Boundary conditions are the conditions existing at the physical boundary of the domain. In stress analysis problem, they refer to displacements or rotation and forces/ moment conditions. Since the upper part of the ultrasonic tool is fixed in the horn, therefore no longitudinal movements and no rotational movements are allowed. The boundary conditions were imposed to finite element model by freezing all degrees of freedom of motion at one end (ENCASTRE; U1=U2=U3=UR1=UR2=UR3=0). The same condition was applied to the work piece which was held at the base. The displacement was provided to the abrasive particle. This energy transfer to abrasive particles force the particles to strike with the work material at a high velocity of approximately 750 m/s. The mass of the abrasive is assumed to be fixed in all cases, and it is taken as 0.0001 gm.

Basis Geometry of Abrasive Particle, Work Material and USM Tool

Abrasive particles are the most significant component of the traditional ultrasonic as well as chemical assisted ultrasonic machining processes. The material erosion process is a directly related to the abrasive grit size. These abrasive particles don't possess any particular definitive shape. Thus for finite element analysis, spherical shape of abrasive has been assumed as shown in Figure 2. The tetrahedron meshing is recommended for the spherical objects. It has 952 tetrahedron elements.

Polycarbonate bullet proof (UL-752) glass is basically composition of glass and polycarbonate material, in which, number of layers are defined by the impact load bearing capacity. These layers are glued with each other by a clear adhesive material. Figure 3 shows the work material (UL-752) for FEA, it has three layers of glass and two layers of polycarbonate materials. The mechanical properties have been defined appropriately for these materials for carrying out the finite element analysis. Triangular Prism type of meshing is preferred for cube structure. There are total 14400 elements in three layers of glass and 9589 elements in two layers of polycarbonate material.

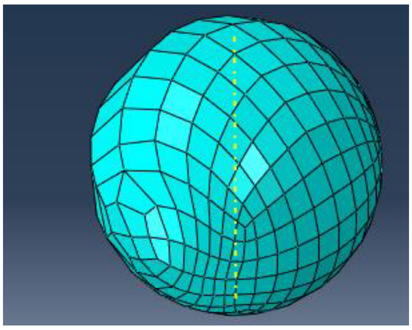

Figure 2: Abrasive Mesh Diagram.

Ultrasonic tool is the important part of ultrasonic machining. The tool material has to bear the 20 kHz – 30 kHz frequency and high power rating. The selection of tool material is a significant factor for precise tool fabrication. The selected tool material must have some important properties like: high resonance resistance, high impact load bare capacity, and high fatigue resistance, etc. Figure 4 shows the USM tool. It has tetrahedron type meshing and 1859 elements.

Assembly

Assembly of work piece and abrasive

Next is assembly of work plate (Polycarbonate bullet proof UL-752 glass) with abrasive particle. The abrasive particle has been shown in the red color sphere. Work material has been depicted by two color plate, brown color showing the polycarbonate material and white color plate representing glass material. Glass and polycarbonate materials have face to face or mesh to mesh interaction. This means it behaves like a single material. Figure 5 shows the assembly of work material and abrasive.

USM tool and abrasive assembly

USM tool never comes into contact with work piece, it transmits its energy onto the abrasive particles. These abrasive particles strike over the work material with intense energy due to intense vibrations produced by the tool and this energy is used to erode the material at the cutting zone. Figure 6 shows the tool and abrasive assembly.

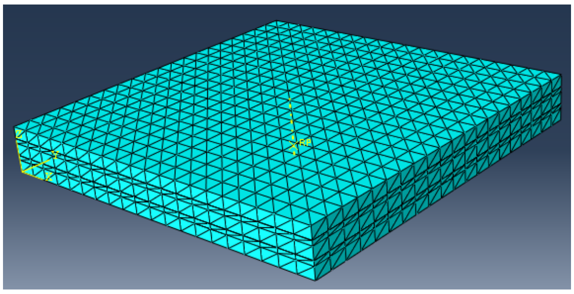

Figure 3: Polycarbonate Bullet Proof (UL-752) Glass Plate.

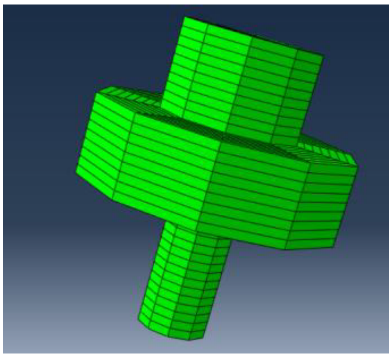

Figure 4: USM Tool.

FEM Analysis and Results Discussion

Alumina (Al_2O_3) abrasive particle and polycarbonate UL-752 glass

Some basic properties of Alumina (Al_2O_3), Silicon Carbide (SiC) and Boron Carbide (B_4C) abrasive has been used for the FEM analysis. Table 1 shows the properties of Al_2O_3, SiC and B_4C particle. Figure 7 shows the FEM analysis of Alumina (Al_2O_3) Particle and Polycarbonate Plate. The cut section of the plate shows that the impact of the abrasive has propagated in longitudinal as well as lateral axis of the plate. The deep red part shows the maximum stress area and blue part shows zero stress area.

32 nodes are affected by the impact of Alumina abrasive, having maximum stress value 3.53e+03 and minimum stress value 3.58e-04. Figure 8 shows the relationship between Operation time and Abrasive ball force, internal resistance of Glass and Plastic displacement of Alumina (Al_2O_3) Particle. The time of operation has been observed in micro seconds. The graph clearly depicts that abrasive ball force or impact energy of abrasive are implemented at the work surface for 0.30 micro seconds. Hardness of the material will oppose the material deformation or erosion process, it also known as the internal resistance property of material.

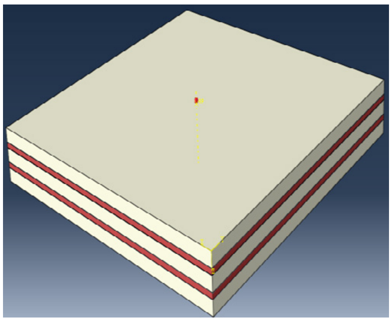

Figure 5: Assembly of work material and abrasive.

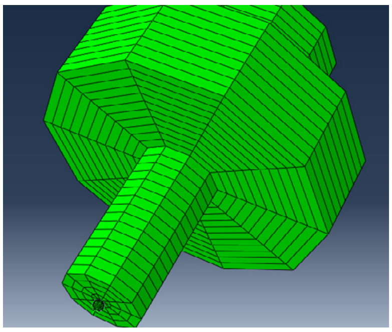

Figure 6: USM tool and Abrasive Assembly.

S.No	Property	Al_2O_3	SiC	B_4C
1.	Density	3.95 g/cm³	4.84 g/cm³	2.55 g/cm³
2.	Melting Point	2072°C	1955°C	2507°C
3.	Boiling Point	2977°C	3204°C	3509°C
4.	Elastic Modulus	300 GPa	1245 MPa	569 MPa
5.	Shear Modulus	124 GPa	51 GPa	195 GPa
6.	Bulk Modulus	165 GPa	176 GPa	271 GPa
7.	Compressive Strength	2100 MPa	1395 MPa	5687 MPa
8.	Poisson's Ration	0.21	0.37	0.21
9.	Hardness	1175 Kg/mm³	3800 MPa	44100 MPa

Table 1: The properties of Al_2O_3, SiC and B_4C particle.

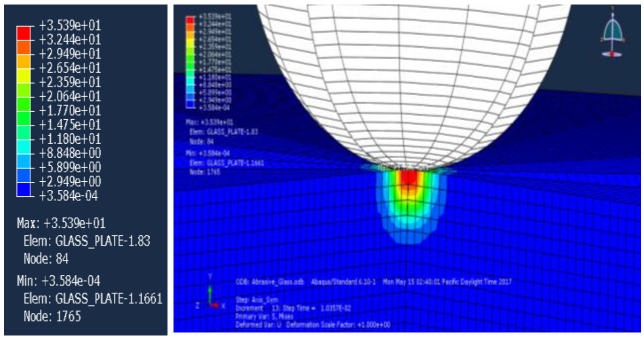

Figure 7: Magnitude of forces generated by Alumina (Al_2O_3) Particle on work surface.

Silicon carbide (SiC) particle and polycarbonate glass

Figure 9 shows the FEM analysis of Silicon Carbide (SiC) abrasive particle and Polycarbonate bullet proof glass. The cut section of the plate shows that the impact of the abrasive has been propagated in longitudinal as well as lateral axis of the plate. As compared to Alumina, SiC abrasive produced large longitudinal stress area. It shows that the SiC abrasive gives deeper impact at the cutting zone and it also gives the better material removal rate as compared to Alumina.

82 nodes are affected by the impact of Silicon Carbide (SiC) abrasive having maximum stress value 5.696e+03 and minimum stress value 3.84e-02. Figure 10 shows relationship between operation time and abrasive ball force, internal resistance of glass and plastic displacement of SiC particle. The time taken to perform the operation is less as compared to Alumina abrasive. It is clear that, SiC abrasive improves the material removal rate. In a short time, it gives the deeper penetration or high longitudinal impact force.

Boron carbide (B_4C) particle and polycarbonate glass

Figure 11 shows the FEM analysis of Boron Carbide (B_4C) Particle and Polycarbonate bullet proof glass. The cut section of the plate shows that the impact of the abrasive has been propagated in longitudinal as well as lateral axis of the plate. As compared to Alumina and Silicon Carbide, it has huge longitudinal as well as lateral stress at the cutting zone. It can be concluded that the B_4C abrasive have deeper impact at the cutting zone and it also gives the much better material removal rate as compare to Alumina and Silicon Carbide abrasive. The deep red part shows the maximum stress area and blue part shows zero stress area.

504 Nodes are affected by the impact of Boron Carbide (B_4C) abrasive having maximum stress value 6.000e+03 and minimum stress value 4.622e-0. Figure 12 shows the interaction between operation time and abrasive ball force, internal resistance of glass and plastic displacement of B_4C abrasive particle. The time taken to perform the operation is less as compared to Alumina and Silicon carbide abrasives. It is therefore evident from the analysis that, B_4C abrasive enhances the material removal rate. In short time, it gives the deeper penetration or high longitudinal and lateral impact forces.

Citation: Singh KJ (2019) Finite Element Analysis of Chemical Assisted Ultrasonic Machining Process to Investigate the Effect of Abrasive on Polycarbonate (UL-752) Glass and USM Tool. J Material Sci Eng 8: 507. doi: 10.4172/2169-0022.1000507

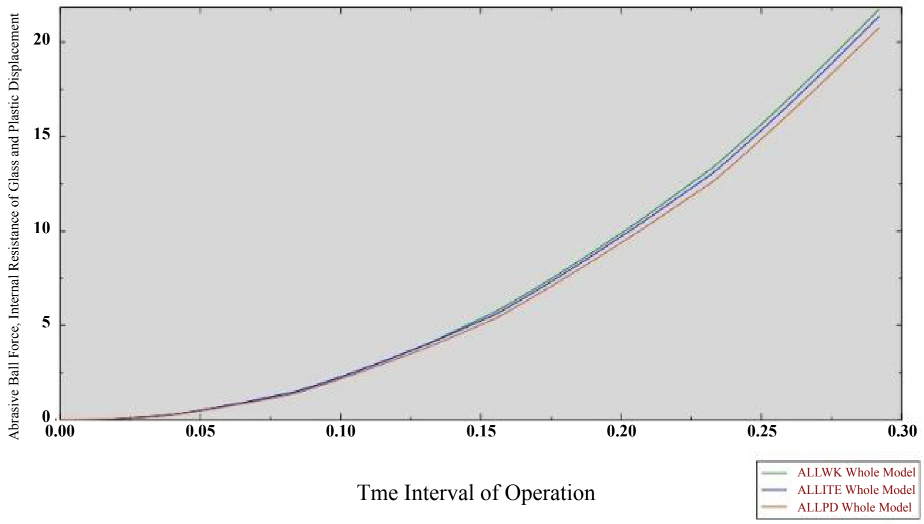

Figure 8: Graph of between Operation time and Abrasive ball force, Internal resistance of Glass and Plastic Displacement of Alumina (Al_2O_3) Particle.

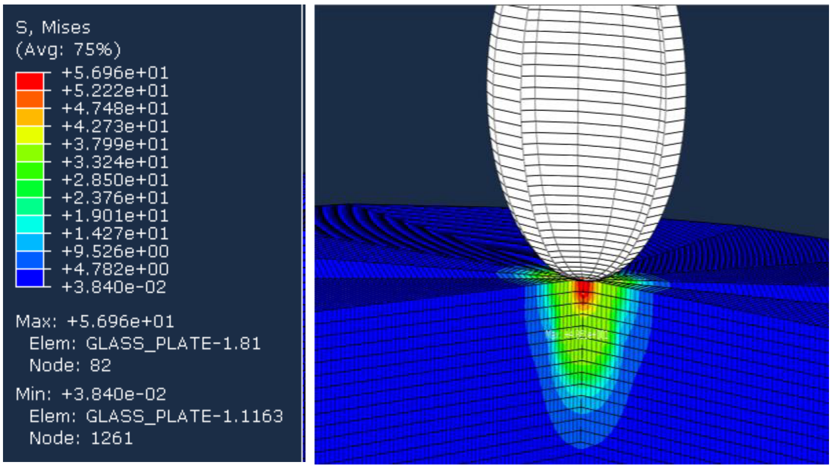

Figure 9: Magnitude of forces generated by Silicon Carbide (SiC) Particle on work surface.

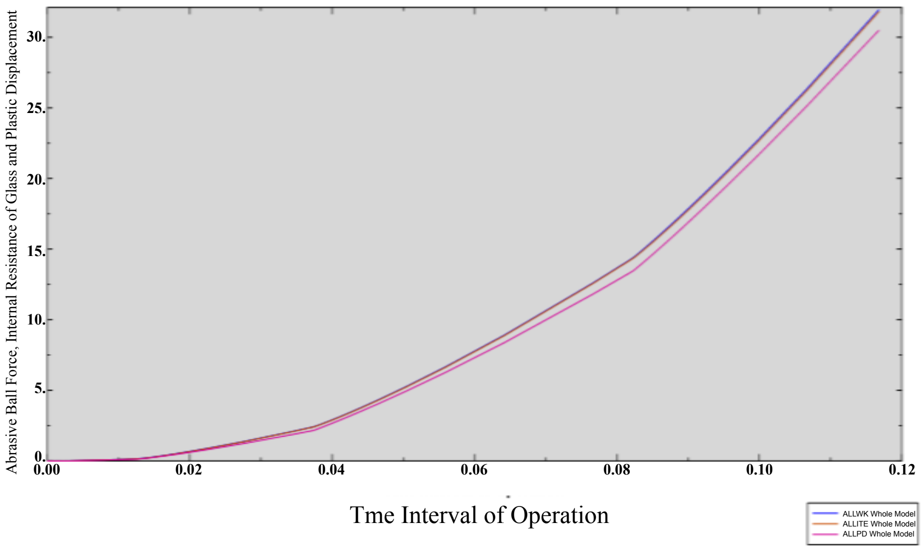

Figure 10: Graph of between Operation time and Abrasive ball force, Internal resistance of Glass and Plastic Displacement of Silicon Carbide (SiC) Particle.

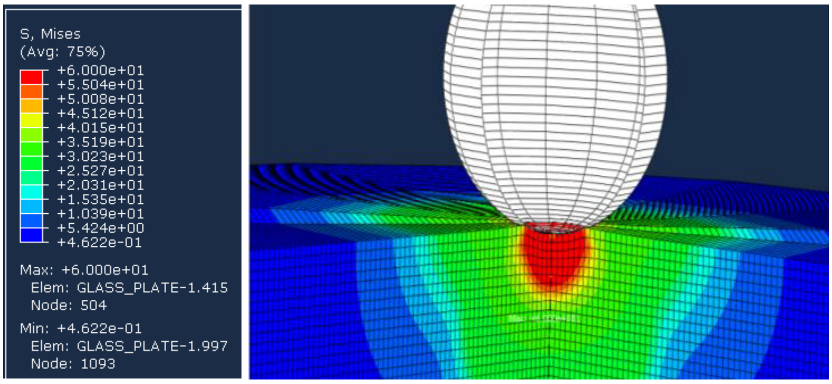

Figure 11: Magnitude of forces generated by Boron Carbide (B_4C) Particle on work surface.

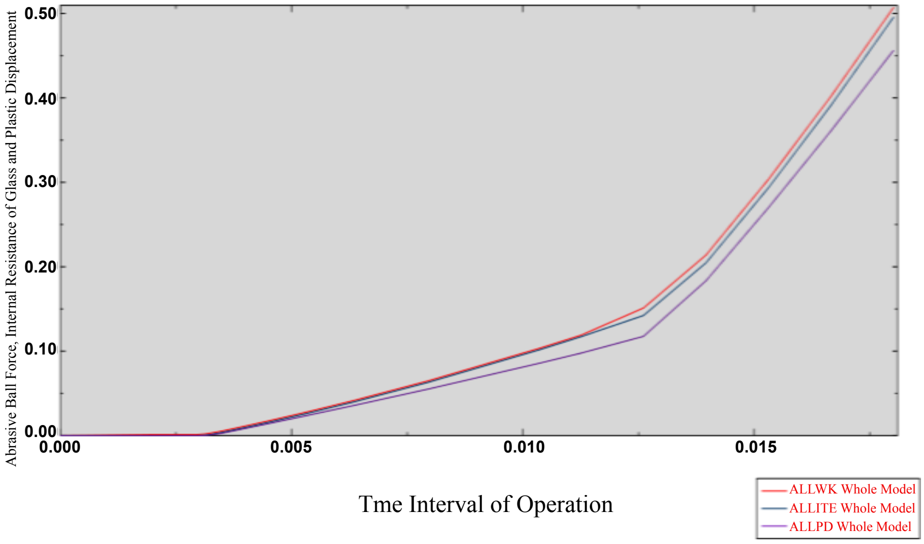

Figure 12: Graph of between Operation time and Abrasive ball force, Internal resistance of Glass and Plastic Displacement of Boron Carbide (B_4C) Particle.

FEM Analysis of Abrasive and High Speed USA Tool and Results Discussion

Al_2O_3 abrasive and high speed steel tool

Abrasive particles flows in between the tool and work-piece through carrier medium. Ultrasonic machine tool has longitudinal direction movement. When tool vibrates with ultrasonic frequency (20 kHz to 30 kHz), the abrasive particles are forced to move towards the work piece, at same time these abrasive particles are produce the impact at tool surface. They also remove the material from the tool surface, generally known as tool wear. The harder abrasive particles give high tool wear rate and reduce the tool life. Figure 13 shows the FEM analysis of Alumina Al_2O_3 abrasive and High Speed Steel Tool. The maximum value of impact energy is 4.01e+1 and minimum value is 5.12e-03.

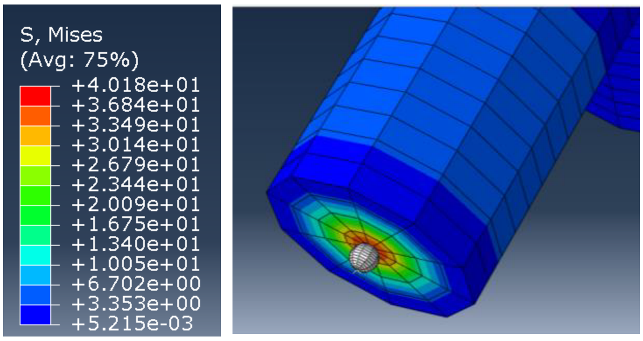

Figure 13: Magnitude of forces and enlarged view of Al_2O_3 and High Speed Steel Tool.

The graph of V-Mises stresses versus longitudinal axis of tool is shown in Figure 14. It shows that the impact of stress or energy gets reduced along the longitudinal axis. Thus longitudinal stresses are reduced toward the longitudinal axis.

SiC and high speed steel tool

Figure 15 shows the FEM analysis of Silicon Carbide (SiC) and High Speed Steel Tool. The maximum value of impact energy is 5.19e+1 and minimum value is 6.11e-03. Same boundary conditions are used for the FEM analysis as in the previous case of Al_2O_3 abrasive. SiC abrasive produce the more impact as compared to Al_2O_3 abrasive. SiC abrasive gives the high tool wear rate as compared to Al_2O_3 abrasive. Figure 15 also shows that SiC abrasive produces more longitudinal and lateral stress at the abrasive striking zone. It has been observed that SiC

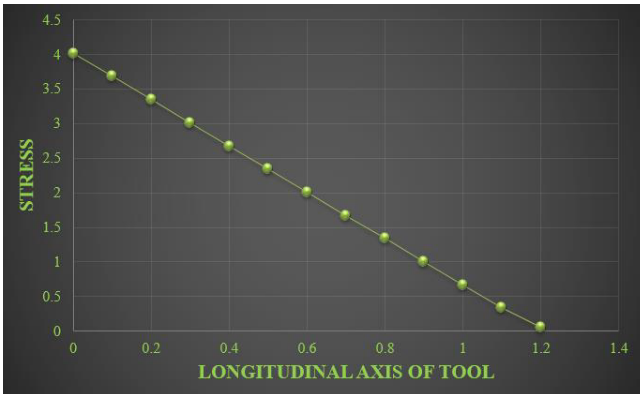

Figure 14: V.Mises stresses analysis graph for Al_2O_3 abrasive and High Speed Steel Tool.

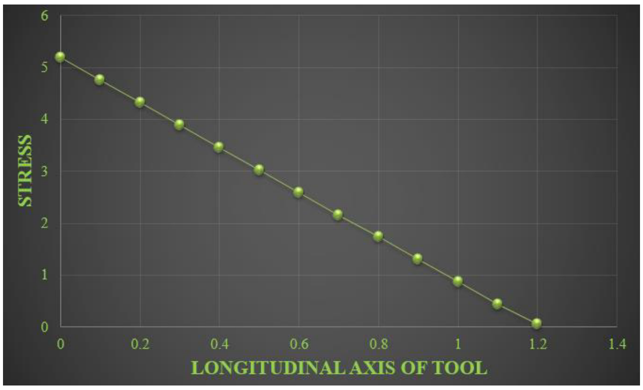

Figure 16: V.Mises stresses analysis graph for SiC abrasive and High Speed Steel Tool.

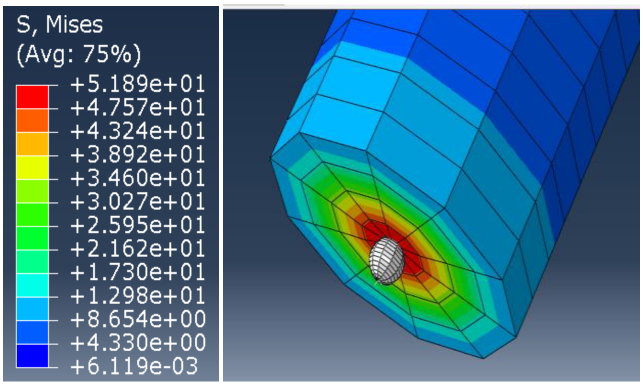

Figure 15: Magnitude of forces and enlarged view of SiC and High Speed Steel Tool.

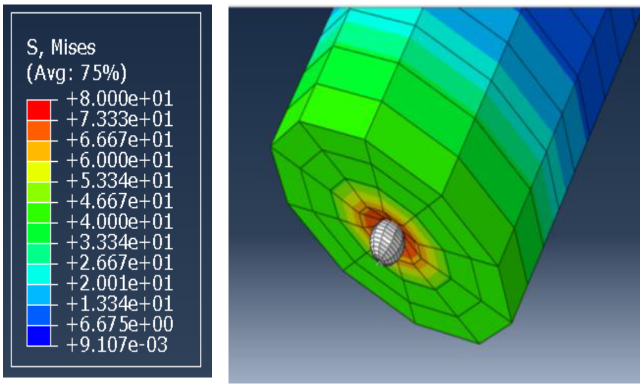

Figure 17: Magnitude of forces and enlarged view of B_4C and High Speed Steel Tool.

abrasive gives high tool wear rate and lower tool life as compared to Al_2O_3 abrasive.

Figure 16 shows the Graph of V-Mises stresses versus longitudinal axis of tool. It shows that the impact of stress or energy gets reduced along the longitudinal axis. Thus longitudinal stresses are reduced toward the longitudinal axis.

B_4C and high speed steel tool

Figure 17 shows FEM analysis of B_4C and High Speed Steel Tool. The maximum value of impact energy is 8.00e+1 and minimum value is 9.10e-03. Under same boundary conditions, B_4C abrasive has the more impact on machining zone as compared to SiC and Al_2O_3 abrasives. B_4C abrasive gives the high tool wear rate as compared to SiC and Al_2O_3 abrasive, because, B_4C abrasive is a harder abrasive as compared to SiC and Al_2O_3 abrasive.

Figure 17 also shows that B_4C abrasive produces more longitudinal and lateral stress at the abrasive striking zone of tool. B_4C abrasive gives higher tool wear and lower tool life as compared to SiC and Al_2O_3 abrasive. Figure 18 shows the interaction of V-Mises stresses versus longitudinal axis of USM tool. It shows that the impact of stress or energy gets reduced along the longitudinal axis. Thus longitudinal stresses are reduced toward the longitudinal axis.

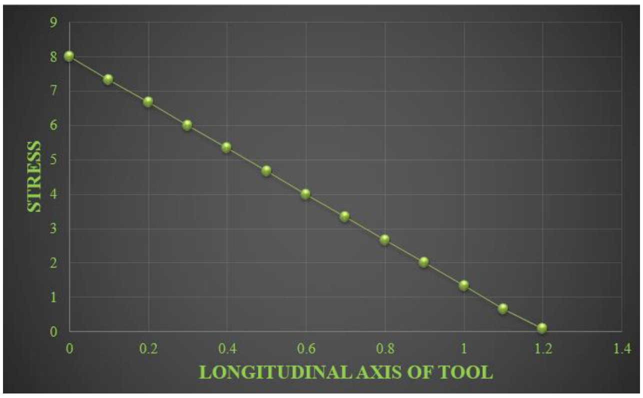

Figure 18: V.Mises stresses analysis graph for B_4C abrasive and High Speed Steel Tool.

Experimentation Results

For the validation of FEM analysis, experimentation has been performed by Alumina (Al_2O_3), Silicon Carbide (SiC) and Boron Carbide (B_4C) abrasives. For machining, setting has been preferred for investigation was 20% concentration, 40% power rating, 280 grit size, water carrying medium, Frequency 20 kHz, static load 1.63 kg, amplitude of vibration 25.3-25.8 μm, Slurry Temperature 25°C and Slurry Flow rate 30 liter/min. Figures 19 and 20 show the comparative results of MRR, TWR with FEM analysis and experimentation. It found that the Experimentation results and FEM analysis gives approximately similarly results.

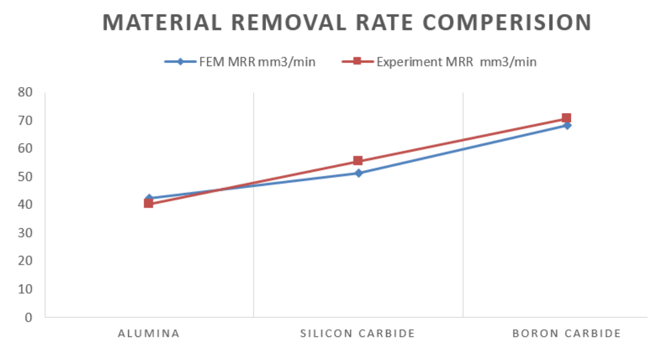

Figure 19: Comparative results of MRR in FEM analysis and experimentation.

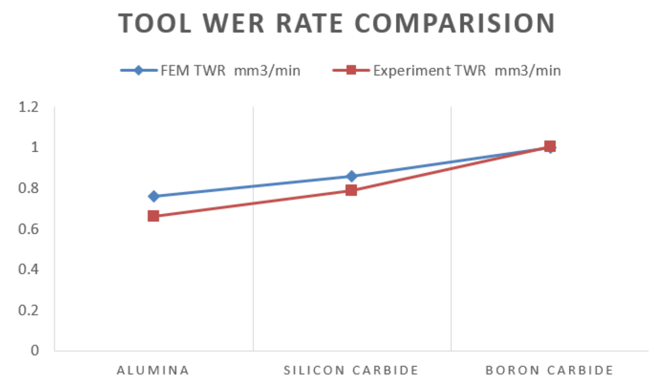

Figure 20: Comparative results of TWR in Fem analysis and experimentation.

Conclusion and Results of FEM Analysis

1. Finite element analysis of abrasives (Al_2O_3, SiC, and B4C) and polycarbonate bulletproof (UL-752) glass reveals that, harder abrasive leads to higher longitudinal and lateral stresses.
2. B4C abrasive should be preferred for better material removal rate as compared to SiC and Al_2O_3. From the economical point of view, B4C has been found to be more expansive, than SiC and followed by Al_2O_3.
3. The decreasing order of abrasive effectiveness with respect to material removal rate is B4C > SiC > Al_2O_3. After considering all the constraints, most preferable abrasive has been found to be SiC, because it gives reasonably good material removal rate, as well as it is economical and inexpensive as compared to B4C.
4. Similarly, in abrasives (Al_2O_3, SiC, and B4C) and USM tool FEM analysis, it is observed that harder abrasive gives high tool wear rate. In general, the higher material removal rate higher will be the tool wear rate and visa versa.
5. Al_2O_3 abrasive produces lower tool wear rate, but it also produces lower material removal rate. The increasing order of tool wear rate with respect to abrasive is Al_2O_3>SiC> B4C.
6. From both FEM analysis, the preferred abrasive is SiC, because it gives reasonably good material removal rate as well as tool wear rate. Moreover it is inexpensive as compared to B4C abrasive.

References

1. Lia ZC, Liang-Wu Caib ZJ, Peia C (2006) Treadwellc Edgechipping reduction in rotary ultrasonic machining of ceramics:Finite element analysis and experimental verification. Int J Mach Tool Manu 46: 1469-1477.
2. Aminia S, Soleimanimehra H, Nategha MJ, Abudollahb A, Sadeghia MH (2008) FEM analysis of ultrasonic-vibration-assisted turning and the vibratory tool. J Mater Process Technol 201: 43-47.
3. Yu Liua B, Lijun Wanga B, Dongpo Wanga B (2011) Finite element modeling of ultrasonic surface rolling process. J Mater Process Technol 211: 2106-2113.
4. Jain NK, Jain VK (2001) Modeling of material removal in mechanical type of advanced machining processes-a state of the art review. Int J Mach Tool Manu 41: 1573-1635.
5. Jain VK (2013) Advanced Machining Processes. Allied publishers private limited: New Delhi, India.
6. Kumar J (2013) Ultrasonic machining-a comprehensive review. Mach Sci Technol 17: 325-379.
7. Azarhoushang B, Akbari J (2007) Ultrasonic assisted drilling of Inconel 738-LC. Int J Mach Tool Manu 47: 1027-1033.
8. Komaraiah M, Narasimha Reddy PN (1993) A study on the influence of work-piece properties in ultrasonic machining. Int J Mach Tool Manu 33: 495-505.
9. Haslehurst M (1981) Manufacturing Technology. 3rd edn, Viva Book, New Delhi pp: 270-271.
10. Dvivedi A, Kumar P (2007) Surface quality evaluation in ultrasonic drilling through the taguchi technique. Int J Adv Manuf Technol 34: 131-140.
11. Gauri SK, Chakravorty R, Chakraborty S (2011) Optimization of correlated multiple responses of ultrasonic machining (USM) process. Int J Adv Technol 53: 1115-1127.
12. Gilmore R (1991) Ultrasonic machining-a case study. J Mater Process Technol 28: 139-148.
13. Thoe TB, Aspinwall DK, Wise MLH (1998) Review on ultrasonic machining. Int J Mach Tools Manuf 38: 239-255.
14. Neugebauer R, Stoll A (2004) Ultrasonic application in drilling. J Mater Process Technol 149: 633-639.
15. Ghahramani B, Wang ZY (2001) Precision ultrasonic machining process: A case study of stress analysis of ceramic (Al_2O_3). Int J Mach Tool Manu 41: 1189-1208.
16. Goetze D (1956) Effect of vibration amplitude, frequency, and composition of the abrasive slurry on the rate of ultrasonic machining in ketos tool steel. J Acoust Soc Am 28: 1033-1045.
17. Weilong C, Zhijian P (2013) Process of Ultrasonic Machining. Handbook of manufacturing Engineering and Technology, London.
18. Kennedy DC, Grieve RJ (1975) Ultrasonic machining-a review. The Production Engineer 54: 481-486.
19. Rao RV, Pawar PJ, Davim JP (2010) Parameter optimization of ultrasonic machining process using nontraditional optimization algorithms. Mater Manuf Processes 25: 1120-1130.
20. Choi JP, Jeon BH, Kim BH (2007) Chemical-assisted ultrasonic machining of glass. J Mater Process Technol 191: 153-156.
21. Zhang C, Cong W, Feng P, Pei Z (2014) Rotary ultrasonic machining of optical K9 glass using compressed air as coolant: A feasibility study. Proc Inst Mech Eng, Part B 228: 504-514.
22. Sahay C, Ghosh S, Kammila HK (2011) Analysis of ultrasonic machining using monte carlo simulation. Proc ASME Int Mech Eng Congr Expo, Denver: USA.
23. Wiercigroch M, Neilson RD, Player MA (1999) Material removal rate prediction for ultrasonic drilling of hard materials using an impact oscillator approach. Phys Lett 259: 91-96.
24. Bekrenev NV, Muldasheve GK, Petrovskii AP, Tsvetkova OA (2015) Influence of the thermal effect on the cutting forces in the ultrasonic machining of high strength material. Russian Engineering Research 35: 758-759.
25. Nair EV, Ghosh AA (1985) Fundamental approach to the study of mechanics of ultrasonic machining. Int J Prod Res 23: 731-753.
26. Thoe TB, Aspinwall DK (1999) Combined ultrasonic and electric discharge machining of ceramic coated nickel alloy. J Mater Process Technol 92: 323-328.